Sufitri et al. *IJDM (2024) 7:3, pp 231-250*
DOI: https://doi.org/10.24815/ijdm.v7i3.40546

International Journal of
Disaster Management
E-ISSN: 2527-4341 P-ISSN: 2808-439X

RESEARCH ARTICLE Open Access

# Modeling the Dispersion of Air Pollution Due to Volcanic Eruptions

Yumita Sufitri[1], Vera Surtia Bachtiar*[1], Alqadri Asri Putra[1], and Sugeng Nugroho[2]

[1] Environmental Engineering, Andalas University, Indonesia.

[2] Global Atmosphere Watch Station Kototabang, West Sumatra, Indonesia

***Corresponding author:** verasurtia@eng.unand.ac.id

*Received* 07 August 2024; *Received in Revised Form* 20 December 2024; *Accepted* 21 December 2024

**Abstract**

The eruption of Mount Marapi has caused damage to agricultural land and the temporary closure of Minangkabau International Airport. Simulations were conducted using HYSPLIT to detect the initial direction of volcanic ash dispersion. The trajectory analysis from HYSPLIT indicated that the volcanic ash dispersion on December 3, 2023, and January 5, 2024, extended beyond 100 km, while on December 22, 2023, January 19, February 4, and February 23, 2024, the dispersion was less than 100 km. HYSPLIT models indicated that the ash dispersion was directed towards Minangkabau Airport during the closure period. As a result, HYSPLIT can be considered a suitable software for simulating volcanic ash dispersion. Concentration evaluations based on Government Regulation No. 22 of 2022 revealed that several areas exceeded the applicable air quality standards. Validation using data from the HIMAWARI satellite and NASA WorldView indicated similar dispersion direction patterns in the simulation results. However, the Mann-Whitney test revealed significant differences when comparing the concentration outputs from HYSPLIT to PM2.5 levels before and during the eruption, based on PM2.5 monitoring documents from GAW Kototabang. Recommended mitigation measures include prioritizing the volcanic ash hazard zone within a 0-10 km radius from the crater by restricting activities and planning evacuation routes and safe areas away from volcanic ash exposure.

Keywords: dispersion; modelling; pollutant; himawari; marapi

## Introduction

Mount Marapi is one of the active volcanoes in Sumatra that has experienced continuous eruptions from early 2023 to March 2024. It is located in the Agam and Tanah Datar districts and reaches 2,891 meters above sea level. Marapi is one of the most eruptive volcanoes in Sumatra, with over 500 eruptions recorded since 1770 (Center for Volcanology and Geological Hazard Mitigation (PVMBG), 2011) and is intensively monitored by the local Volcano Observation Post (PGA). According to information from the Center for Volcanology and Geological Hazard Mitigation (PVMBG), the eruption column of Mount Marapi can reach altitudes of 75 to 3,000 meters above the crater. The volcano was on alert status (level II) from August 3, 2011, to January 8, 2023 (Putra, 2016; Santoso, 2023). However, since January 9, 2024, volcanic activity has significantly increased, as evidenced by recorded eruption tremors, prompting an upgrade to level III (Standby) status (Center for Volcanology and Geological Hazard Mitigation (PVMBG), 2024).

The eruption of Mount Marapi has caused significant damage, including the destruction of over 900 hectares of agricultural land, affecting 3,000 farmers in the surrounding areas. Additionally, the operational capacity of Minangkabau International Airport (BIM) had to be suspended twice, on December 22, 2023, and January 5, 2024, due to the threat of volcanic ash, resulting in 44 canceled flights (Directorate General of Civil Aviation (DJPU), 2024). Air Quality Monitoring data for PM2.5 from the Global Monitoring Station (GAW) Koto Tabang (2023-2024) recorded a significant increase in PM2.5 concentration before and during the eruption, indicating the impact of volcanic ash on air quality.

Volcanic ash refers to particles emitted by a volcano with a diameter of <4 µm, fragmented from explosive eruptions (Cashman & Rust, 2016). Ash can be produced during various eruption processes and may contain particles that can enter the lungs, posing risks to individuals with pre-existing lung conditions, such as asthma, when exposed to fine ash fall (Horwell *et a.,*2006). As a mitigation effort against the negative impacts of volcanic ash post-eruption, using protective masks for affected communities is one proactive measure. Early detection of volcanic ash dispersion through accurate predictions is essential to minimize the losses caused by the eruption of Mount Marapi.

One method that can be used is the simulation of volcanic ash dispersion through air quality modeling software. This study focuses on using HYSPLIT software for volcanic ash dispersion simulations. HYSPLIT (Hybrid Single-Particle Lagrangian Integrated Trajectory) is a widely used software for simulating atmospheric pollutant dispersion (Fleming et al., 2012). It is one of the most used atmospheric transport and dispersion models in the atmospheric science community. A study using HYSPLIT to simulate ash dispersion from Mount Sakurajima in Japan showed a 63.52% match between the model's ash dispersion path and satellite data from COMS-GOCI, yielding satisfactory results (Lee *et al*., 2014).

The GAW Kototabang Station, as an atmospheric observation institution, has been using the online version of HYSPLIT with default data from the Global Data Assimilation System (GDAS), which has a spatial resolution of 1 degree (Rodell *et al*., 2004). However, using GDAS datasets can result in significant differences in simulations, particularly regarding the vertical velocity calculation method. Therefore, using the offline version of HYSPLIT with higher-resolution meteorological data could be considered a more accurate alternative (Su *et al.*, 2015).

In addition to HYSPLIT, this study also involves validation using data from the HIMAWARI-8 satellite and PM2.5 concentration data obtained from GAW Kototabang's air quality monitoring documents. HIMAWARI-8 is used to validate volcanic ash dispersion patterns, as this geostationary weather satellite managed by Japan is equipped with imaging sensors that continuously monitor Earth Day and night over the Western Pacific region. The satellite provides real-time data for weather forecasting, tropical storm monitoring, volcanic activity detection, and volcanic ash dispersion. Moreover, Himawari is utilized for monitoring air pollutants such as PM2.5 and hazardous gases and in air quality studies, as well as being crucial for natural disaster monitoring and atmospheric research (Japan Aerospace Exploration Agency Earth Observation Research Center (JAXA EORC), 2018).

The main goal of this research is to compare the volcanic ash dispersion simulation results using HYSPLIT with observation data from HIMAWARI-8 to assess the accuracy and efficiency of the HYSPLIT model in predicting the dispersion of ash from the eruption of Mount Marapi. Additionally, the results of this study are expected to provide valuable insights for developing more effective early warning systems to assist in disaster mitigation efforts and managing the impacts of eruptions on communities and the environment.

*Meteorological Condition*

The dispersion of pollutants is closely related to the meteorological conditions surrounding the pollution source. Meteorological data required as input for the HYSPLIT software includes six-hour interval data at 00:01, 06:00, 12:00, 18:00, and 00:00, covering meteorological parameters such as wind direction and speed, as well as radiation, as presented in Table 1 below:

Table 1. Meteorological Conditions Around the Site At The Time Of The Eruption

| Time | Hours | Wind Speed (m/s) | Wind Direction (degrees) | Solar Radiation (W/m$^2$) |
|---|---|---|---|---|
| 23/12/03 | 01.00 | 1,4 | 228,8 | 0 |
| | 06.00 | 1,4 | 270,7 | 0 |
| | 12.00 | 1,6 | 200,8 | 596,3 |
| | 18.00 | 0,9 | 257,0 | 50,4 |
| | 24.00 | 1,0 | 236,0 | 0 |
| 23/12/22 | 01.00 | 0,7 | 46,9 | 0,0 |
| | 06.00 | 1,1 | 334,5 | 31,4 |
| | 12.00 | 2,4 | 35,3 | 613,1 |
| | 18.00 | 1,0 | 44,7 | 0,0 |
| | 24.00 | 0,5 | 337,5 | 0,0 |
| 24/01/05 | 01.00 | 1,0 | 38,4 | 0,0 |
| | 06.00 | 0,5 | 353,5 | 21,3 |
| | 12.00 | 2,8 | 27,9 | 663,3 |
| | 18.00 | 1,6 | 30,7 | 8,3 |
| | 24.00 | 1,2 | 312,6 | 0,0 |
| 24/01/19 | 01.00 | 0,9 | 302,8 | 0,0 |
| | 06.00 | 1,0 | 332,3 | 0,0 |
| | 12.00 | 1,6 | 20,1 | 635,0 |
| | 18.00 | 0,5 | 274,9 | 106,6 |
| | 24.00 | 0,8 | 217,6 | 0,0 |
| 24/02/04 | 01.00 | 1,3 | 255,54 | 0,0 |
| | 06.00 | 1,4 | 242,87 | 0,0 |
| | 12.00 | 1,8 | 283,73 | 825,6 |
| | 18.00 | 2,0 | 253,43 | 160,3 |
| | 24.00 | 1,4 | 236,57 | 0,0 |
| | 01.00 | 1,2 | 265,9 | 0,0 |
| | 06.00 | 1,5 | 241,1 | 0,0 |
| 24/02/23 | 12.00 | 1,6 | 237,8 | 768,7 |
| | 18.00 | 1,2 | 243,8 | 41,2 |
| | 24.00 | 1,5 | 225,9 | 0,0 |

Source: NASA Langley Research Center, 2023 & 2024

*Volcanic Activity*

Mount Marapi is a volcano in West Sumatra, Indonesia (Figure 1). It is classified as one of the most active volcanoes in Sumatra and is geographically situated at 0° 22' 47.72" S, 100° 28' 16.71" E. Administrative-ly, it is located in Agam Regency. The view of Mount Marapi can be observed from the cities of Bukittinggi, Padang Panjang, and Tanah Datar Regency, with an elevation reaching 2,891 meters (Hamdiyessi *et al.*, 2022).


**Figure 1.** Mount Marapi Location Map
**Source:** PVMBG, 2023
.

According to the Volcanic Contingency Document for West Sumatra from 2016, Mount Marapi is classified as a stratovolcano, characterized by its conical layered structure and both effusive and explosive eruption types, marked by booming sounds during eruptions. This volcano is formed from the extrusion of viscous lava (Suhendro *et al*., 2022). It contains five craters (Iqbal *et al*., 2023): Kaldera Bancah (A), Kapundan Tuo (B), Kabun Bungo (C), Kapundan Bongso (D), and Kawah Verbeek (D4), as well as a fumarole field named Sibangor Julu.

From 2011 to early 2014, Mount Marapi's activity increased, culminating in an alert status on February 26, 2014, and necessitating a 3 km evacuation. On December 3, 2023, a significant eruption sent ash 3,000 meters high, causing local ashfall, air pollution, and 24 climber deaths (Center for Volcanology and Geological Disaster Mitigation (PVMBG), 2023). From 2011 to early 2014, Mount Merapi's activity increased, culminating in an alert status on 26 February 2014 and necessitating a 3 km evacuation. On 3 December 2023, a significant eruption sent ash 3,000 meters high, causing local ashfall, air pollution, and 24 climber deaths (Ministry of Energy and Mineral Resources (ESDM), 2023).

Based on observational data of Mount Marapi's activity recorded between November 2023 and February 2024 by the Center for Volcanology and Geological Hazard Mitigation available on the website http://magma.esdm.go.id as shown in Table 2, an eruption with a high ash column, it occurred on 3 December 2023, with an ash column height of approximately 3,000 meters from the crater. The lowest ash column was observed on 4 February 2024, with a height of 100 meters from the crater. In November 2023, Mount Marapi was observed to emit only smoke puffs from the crater. The diameter of Verbeek Crater was measured using Google Earth digitization, resulting in a diameter of 0.69 km. Air dispersion modeling was conducted on December 3 and 22, 2023, January 5 and 19, 2024, and February 4 and 23, 2024.

Table 2. Eruption Activity Input Data

| No | Date | Consideration | Eruption Height |
|---|---|---|---|
| 1. | 3/12/ 23 | Highest eruption height | 3000 |
| 2. | 22/12/23 | BIM closure due to eruption | 500 |
| 3. | 5/01/24 | BIM closure due to eruption | 500 |
| 4. | 19/01/24 | BIM closure due to eruption | 500 |
| 5. | 4/02/24 | Lowest eruption height | 500 |
| 6. | 23/02/24 | The most frequent eruption height | 500 |

Source: MAGMA Indonesia (2023 & 2024)

## Methods

The research began with observations and preliminary studies to obtain secondary data by analyzing general information and activities related to the pollutant source, namely Mount Marapi, and determining the coordinates of the pollutant source location. Data observation was also conducted at several relevant institutions to gather available data related to the study. This research collected information from scientific publications, government databases, and previous studies. Meteorological data were sourced from the Global Atmosphere Watch (GAW) station in Bukit Kototabang and NASA Power Satellite Data. These datasets included meteorological parameters such as wind direction and speed, mixing height, and atmospheric stability.

According to Hemond & Fechner (2015), Mixing height is influenced by atmospheric stability, where higher mixing heights typically indicate more unstable conditions and a more significant potential for pollutant dispersion. The determination of the mixing height was calculated using the equation provided by Arya (2005):

$$h = \frac{0.3u*}{f} \quad (1)$$

Where:
u∗: Shear velocity
*f*: Coriolis parameter

The input data pertain to atmospheric stability, influenced by vertical air movement caused by temperature and pressure, triggering convection or air mixing. Earth's heating through conduction and convection affects air conditions, leading to horizontal, vertical, and turbulent motion. Thermal turbulence occurs due to solar heating, while mechanical turbulence arises from obstacles. High atmospheric stability can enhance pollutant dispersion; however, mechanical turbulence can impede airflow and increase pollutant concentrations (Franek & De Rose, 2003). A widely used atmospheric stability classification is the Pasquill-Gifford stability categories, which are determined based on wind speed measured 10 meters above ground level. These categories are classified as follows: A (very unstable), B (moderately unstable), C (slightly unstable), D (neutral), E (slightly stable), and F (stable) (Kahl & Chapman ,2018). In Table 3, the following are the results of the analysis of the meteorological data.

Table 3. Results of Mixing Heights and Atmospheric Stability Analysis

| Time | Hours | Mixing Height (meter) | Atmospheric Stability |
|---|---|---|---|
| 23/12/03 | 01.00 | 457,6 | F |
| | 06.00 | 432,0 | B |
| | 12.00 | 508,9 | B |
| | 18.00 | 278,4 | B |
| | 24.00 | 307,2 | F |
| 23/12/22 | 01.00 | 220,8 | F |
| | 06.00 | 358,4 | B |
| | 12.00 | 761,7 | B |
| | 18.00 | 329,6 | B |
| | 24.00 | 144,0 | F |
| 24/01/05 | 01.00 | 310,4 | F |
| | 06.00 | 153,6 | B |
| | 12.00 | 896,1 | B |
| | 18.00 | 508,9 | B |
| | 24.00 | 374,4 | F |
| 24/01/19 | 01.00 | 275,2 | F |
| | 06.00 | 326,4 | F |
| | 12.00 | 508,9 | A |
| | 18.00 | 144,0 | B |
| | 24.00 | 262,4 | F |
| 24/02/04 | 01.00 | 409,6 | F |
| | 06.00 | 454,4 | F |
| | 12.00 | 560,1 | A |
| | 18.00 | 630,5 | C |
| | 24.00 | 457,6 | F |
| 24/02/23 | 01.00 | 384,0 | F |
| | 06.00 | 470,5 | F |
| | 12.00 | 521,7 | A |
| | 18.00 | 368,0 | B |
| | 24.00 | 473,7 | F |

Source: Research Result (2024)

Another input data source is the pollutant rate. For pollutant sources from volcanic eruptions, the mass eruption rate (MER) measures the intensity of a volcanic eruption by calculating the amount of volcanic material ejected per unit of time. The Mastin relationship links MER to the height of the ash plume, which is crucial for estimating eruption rates. Recent research uses a database of 134 volcanic events to improve this empirical relationship. The Mastin relationship also includes prediction intervals to estimate uncertainty. MER estimates are helpful in classifying the size and intensity of eruptions and forecasting the dispersion of ash and volcanic gases, which is essential for hazard assessment and risk management (Mastin, 2009). The eruption rate (kg/s), As shown in Table 4, can generally be estimated based on observations of the eruption ash column using the equation (Mastin *et al*., 2014):

$$M_{Empir} = 140 \times Hobs\ (km)^{4,15} \qquad (2)'$$

Where:
$M_{Empir}$ : Eruption rate (kg/s)
Hobs : Ash column height (km)

Table 4. Results of Eruption Rate Analysis

| No | Date | Eruption Height | Eruption Rate (kg/S) |
|---|---|---|---|
| 1. | 3/12/ 23 | 3000 | 420.000 |
| 2. | 22/12/23 | 500 | 70.000 |
| 3. | 5/01/24 | 500 | 70.000 |
| 4. | 19/01/24 | 500 | 70.000 |
| 5. | 4/02/24 | 500 | 70.000 |
| 6. | 23/02/24 | 500 | 70.000 |

Source: Research Result (2024)

### *HYSPLIT Modelling*

The Hybrid Single-Particle Lagrangian Integrated Dispersion (HYSPLIT) model, developed by NOAA's Air Resources Laboratory (ARL), is widely used for calculating atmospheric dispersion. As referenced by Fleming *et al. (2012),* the development of HYSPLIT began with a simple manual and has evolved to include calculations of movement, mixing, chemical reactions, and deposition of pollutants and hazardous materials. It encompasses simulations of atmospheric pollutant emissions, radionuclides, wildfire smoke, volcanic ash, mercury, and particles (Stein *et al.,* 2015).

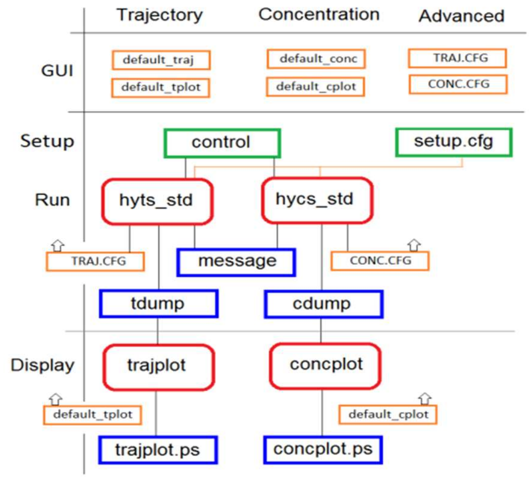


**Figure 2.** HYSPLIT Software Workflow Graph
Source : Stein *et al*, 2015

This model was developed between the 1940s and 1970s to track radioactive debris from Soviet nuclear tests by calculating backward trajectories using radiosonde wind data, with a location error of about 5% (Angell *et al.*, 1972). Over time, it evolved into software that includes interrelated components with specific functions, as shown in Figure 2: the Meteorological Component, Dispersion Component, Concentration Component, and Advanced Component. The HYSPLIT model's calculation method combines Lagrangian and Eulerian approaches. The Lagrangian approach uses a moving reference frame to calculate advection and diffusion as air trajectories or parcels move from their initial locations. In contrast, the Eulerian approach employs a fixed three-dimensional grid as a reference frame to compute pollutant concentration in the air (Draxler *et al.,* 1998).

The volcanic ash dispersion simulation results for Mount Marapi, obtained using the HYSPLIT and AERMOD software, are further evaluated by comparing them with observational data from satellite imagery. This approach aims to ensure the accuracy of the models in representing the dispersion patterns of volcanic ash in the atmosphere, providing a more reliable understanding of the ash's impact on the environment and public health.

*Validation*

Himawari 8

The Meteorological Satellite Center (MSC) of the Japan Meteorological Agency (JMA) has operated the Geostationary Meteorological Satellite (GMS), known as "Himawari," since 1978. Himawari, equipped with advanced imaging sensors, continuously captures Earth Day and night images over the Western Pacific region. These satellite images are used for weather analysis, forecasting, and monitoring abnormal weather conditions, contributing to the prevention and mitigation of natural disasters such as typhoons, heavy rain, and snowstorms (Japan Aerospace Exploration Agency Earth Observation Research Center (JAXA EORC), 2024).

The Himawari satellite is regarded as the successor to the Multifunctional Transport Satellite (MTSAT) series. Its development primarily aims to enhance meteorological observations for disaster preparedness and weather forecasting, improve short-term forecast capabilities, particularly in detecting and predicting severe weather, and advance numerical weather prediction, climate monitoring, and environmental observation. Since 2015, the Indonesian Meteorological, Climatological, and Geophysical Agency (BMKG) has utilized Himawari satellite images to detect volcanic ash using the RGB compositing method (Ishii *et al.*, 2018).

Validation was conducted to assess the correlation between the dispersion patterns generated by the HYSPLIT air modeling software and satellite imagery captured over the West Sumatra region, particularly around Mount Marapi.

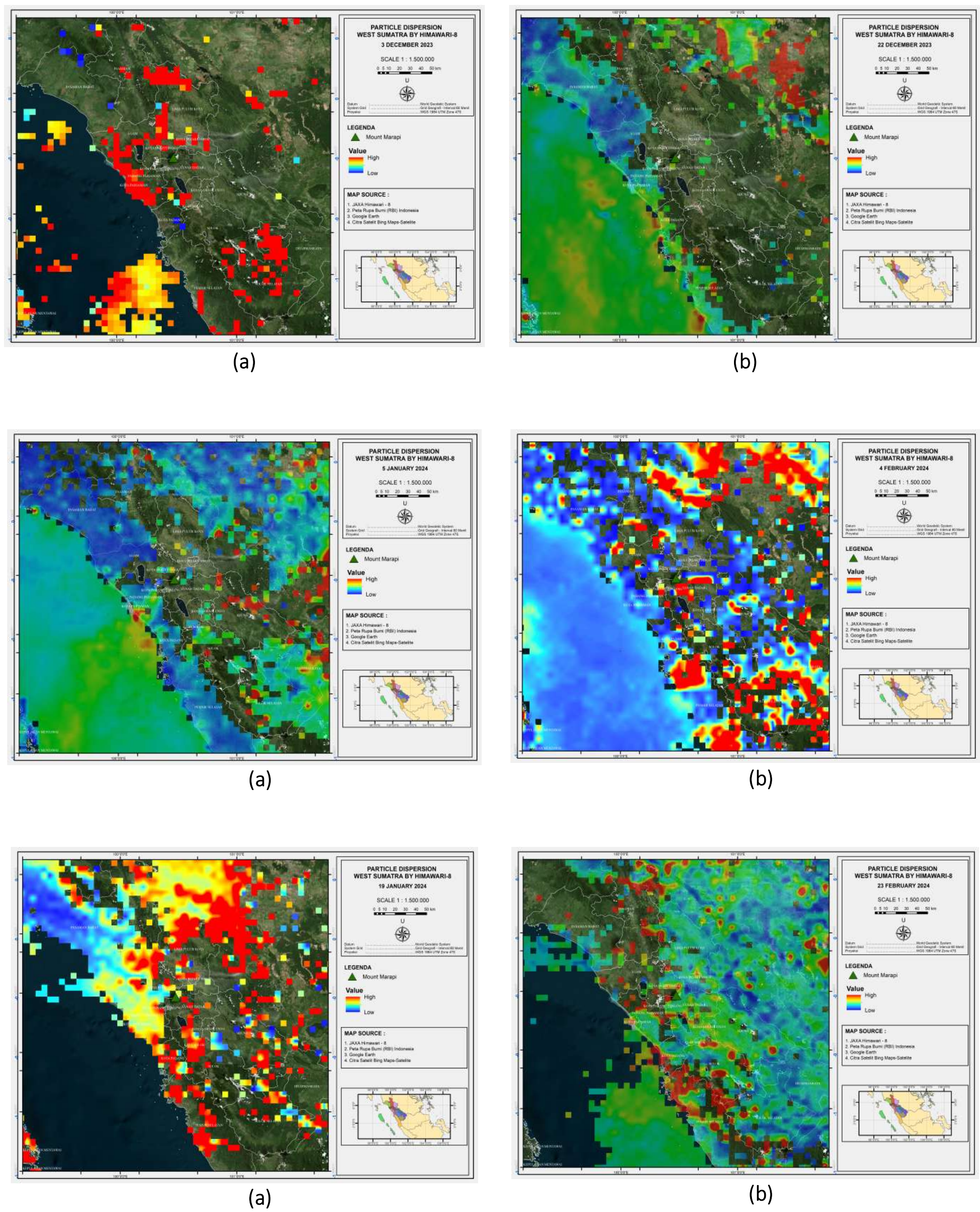


Figure 3. Particle dispersion comparison between Himawari Satellites and HYSPLIT Modelling (a) 3rd December 2023 (b) 22nd December 2023 (c) 5th January 2024 (d) 19th January 2024 (e) 4th February 2024 (f) 23rd February 2024.

Source: Research Results (2024)

The HIMAWARI imagery used in this validation consists of daily satellite images, composites, or averages taken over an entire day. Satellite imagery data from the Meteorological Satellite Center (MSC) of the Japan Meteorological Agency (JMA) or HIMAWARI was visualized using ArcGIS software. The following are the results of the data processing conducted on the Himawari satellite data, as shown in Figure 3.

*Concentration Validation*

The concentration output obtained from the volcanic ash dispersion modeling using HYSPLIT was then compared with PM2.5 concentrations from monitoring data obtained from GAW Kototabang. Table 5 compares the concentrations obtained for each district and city within the modeling area, particularly in regions consistently exposed to volcanic ash. By comparing the HYSPLIT modeling results with data from GAW Bukit Kototabang, we can evaluate the accuracy and reliability of the HYSPLIT in estimating PM2.5 concentrations, thus providing insight into its precision and dependability.

Table 5. Monitoring Data of PM2.5 on the Day Before and During the Modeling Process

| Region | Date | Monitoring Data (µg/m³) | Date | Monitoring H-1 Data (µg/m³) |
|---|---|---|---|---|
| Tanah Datar | 3/12/ 23 | 14,039 | 2/12/ 23 | 10,795 |
| | 22/12/23 | 6,951 | 21/12/23 | 6,518 |
| | 5/01/24 | 12,099 | 4/01/24 | 6,189 |
| | 19/01/24 | 9,021 | 18/01/24 | 6,632 |
| | 4/02/24 | 9,340 | 3/02/24 | 8,803 |
| | 23/02/24 | 9,428 | 22/02/24 | 7,793 |
| Agam | 3/12/ 23 | 16,071 | 2/12/ 23 | 10,023 |
| | 22/12/23 | 6,951 | 21/12/23 | 5,596 |
| | 5/01/24 | 9,255 | 4/01/24 | 8,236 |
| | 19/01/24 | 7,385 | 18/01/24 | 7,217 |
| | 4/02/24 | 5,800 | 3/02/24 | 4,963 |
| | 23/02/24 | 5,504 | 22/02/24 | 5,112 |

Source: GAW Monitoring Data (2023 & 2024)

## Results

*Dispersion By HYSPLIT*

The next step is to populate the dispersion model with the relevant data to visualize volcanic ash dispersion from Mount Marapi. The necessary inputs include meteorological data in "bin" format and parameters such as eruption height, location coordinates, and the event's timing. Additionally, data related to volcanic activity, including eruption rate, specific characteristics being modeled, and the duration of the modeling period, as presented in Tables 3 and 4, must also be included. By integrating all this data, we can conduct.

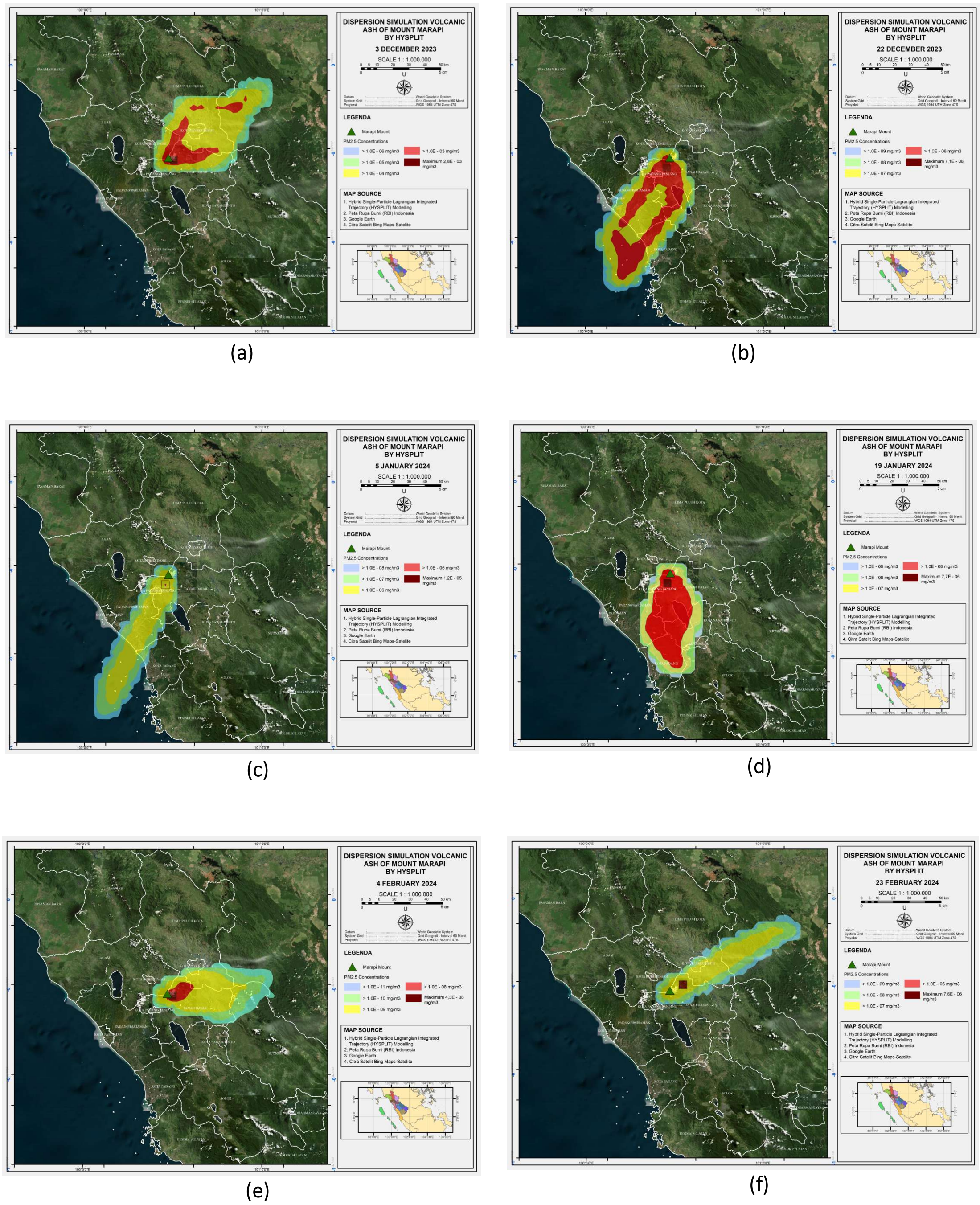


**Figure 4.** Volcanic Ash Dispersion Using HYSPLIT (a) 3rd December 2023 (b) 22nd December 2023 (c) 5th January 2024 (d) 19th January 2024 (e) 4th February 2024 (f) 23rd February 2024

Source: Research Results (2024)

.

Figure 4 (a) – (f) illustrates the simulation of volcanic ash dispersion from Mount Marapi using the HYSPLIT software. The dispersion and concentration of volcanic ash vary daily throughout the modeling period. Figure 4

(a) depicts the dispersion and concentration simulation for 3 December 2023, when the ash column height reached 3000 meters above the crater, dispersing northeast with a maximum concentration of 2,8E-03 mg/m³.

On 22 December 2023, as shown in Figure 4 (b), the volcanic ash dispersion and PM2.5 concentration simulation indicated an eruption height of 500 meters from the crater, with the dispersion direction towards the southwest to the west-southwest and a maximum PM2.5 concentration of 7,1E-06 mg/m³. This pattern is similar to Figure 4 (c), which shows the dispersion and PM2.5 concentration on 5 January 2024, also directed towards the southwest to the west-southwest, with a maximum concentration of 1,2E-05 mg/m³.

The 19 January 2024 simulation map Figure 4 (d) indicates that the volcanic ash spread towards the south to south-southwest with a maximum PM2.5 concentration of approximately 7,7E-06 mg/m³. On 4 February 2024, presented in Figure 4 (e), the ash spread direction was towards the east, with a maximum concentration of 4,3E-08mg/m³.

Figure 4 (f) shows the dispersion and PM2.5 concentration for 23 February 2024; the dispersion direction was identified as northeast to east-northeast with a maximum concentration of 7,6E-06 mg/m³. Figures 4 (b) to 4 (d) show that on the day Minangkabau Airport was closed, the predominant dispersion direction was west-southwest to south, towards the airport.

*Validation*

HIMAWARI 8

On 3 December 2023, during an eruption with an altitude of 3000 m, the Himawari 8 satellite Figure 3. (a) had a particle dispersion predominantly towards the north, west, and east of Mount Marapi. Meanwhile, 22 December 2023 was chosen for modeling due to the temporary closure of Minangkabau International Airport in Figure 3 (b), consistent with the dispersion pattern in HYSPLIT, which showed particles concentrated in Padang Pariaman Regency, Padang City, and Pariaman City, all located to the west of Mount Marapi Figure 4 (b).

On 5 January 2024, particle dispersion using the Himawari 8 satellite Figure 3 (c) showed a predominant spread from the south to the northwest. HYSPLIT predictions also indicated a tendency for dispersion towards the southwest to the west-southwest, like HYSPLIT modeling in Figure 4 (c). On 19 January 2024, Figure 3 (4) shows that particle dispersion by the Himawari 8 satellite predominantly extended from the southwest to the north of Mount Marapi, which is like the predictions made by HYSPLIT, showing the spread reaching Padang Pariaman Regency and Padang City to the west of the source on Figure 4 (d).

Validation of HYSPLIT using the Himawari 8 satellite Figure 3 (e) showed particle dispersion in various directions, including east of Mount Marapi. HYSPLIT also indicated dispersion towards the east, consistent with the satellite imagery, indicating the model's validity in Figure 4 (e). The Himawari 8 satellite in Figure 3 (f) displayed particle dispersion predominantly towards the northeast to south of Mount Marapi, similar to the HYSPLIT software, which showed dispersion towards the northeast to the east-northeast, shown in Figure 4 (f).

Based on the volcanic ash dispersion map generated by HYSPLIT, validated using screenshots from satellite data processing with Himawari 8, it can be concluded that the dispersion obtained from HYSPLIT remains within the range of particle dispersion displayed by the satellite stations. The particle dispersion polygons shown by the Himawari 8 satellite indicate a generally more significant extent than HYSPLIT, as the satellite can capture the entire particle distribution from various anthropogenic and natural pollution sources. In contrast, HYSPLIT modeling only presents volcanic ash dispersion specific to the input source, which is Mount Marapi.

Concentrations

Validation of volcanic ash dispersion simulation results using the HYSPLIT software was conducted to assess and verify the extent to which the obtained concentration results align with monitoring data and the PM2.5

concentration forecasts from the GAW Kototabang station. This study tested PM2.5 concentration data from the HYSPLIT software, comparing it with PM2.5 concentration data found in the Air Quality Monitoring and Forecasting documents from the GAW Kototabang as Table 5. This analysis focused on concentrations in Agam Regency and Tanah Datar Regency, which were consistently exposed to volcanic ash dispersion.

Table 6. Comparison value of HYSPLIT PM2.5 concentration with Kototabang GAW Monitoring document

| Region | HYSPLIT (µg/m³) | Date | Monitoring Data (µg/m³) | Date | Monitoring Data H-1 (µg/m³) | Difference (µg/m³) |
|---|---|---|---|---|---|---|
| Tanah Datar | 50000 | 3/12/ 23 | 14,039 | 2/12/ 23 | 10,795 | 3,244 |
| | 79 | 22/12/23 | 6,951 | 21/12/23 | 6,518 | 0,433 |
| | 100 | 5/01/24 | 12,099 | 4/01/24 | 6,189 | 5,910 |
| | 120 | 19/01/24 | 9,021 | 18/01/24 | 6,632 | 2,389 |
| | 0,12 | 4/02/24 | 9,340 | 3/02/24 | 8,803 | 0,537 |
| | 160 | 23/02/24 | 9,428 | 22/02/24 | 7,793 | 1,635 |
| Agam | 50000 | 3/12/ 23 | 16,071 | 2/12/ 23 | 10,023 | 6,048 |
| | >10 | 22/12/23 | 6,951 | 21/12/23 | 5,596 | 1,355 |
| | >10 | 5/01/24 | 9,255 | 4/01/24 | 8,236 | 1,019 |
| | >10 | 19/01/24 | 7,385 | 18/01/24 | 7,217 | 0,168 |
| | >0,01 | 4/02/24 | 5,800 | 3/02/24 | 4,963 | 0,859 |
| | >10 | 23/02/24 | 5,504 | 22/02/24 | 5,112 | 0,392 |

Source: Research Results (2024)

Table 6 above contains a column indicating the difference between the PM2.5 monitoring data on the modeling day and the previous day's monitoring data. It was done to identify and measure the increase in PM2.5 concentrations before and after the volcanic eruption. The values in this difference column are used as reference values for statistical analysis using the T-test.

| | | Paired Differences | | | | | | | |
|---|---|---|---|---|---|---|---|---|---|
| | | | | | 95% Confidence Interval of the Difference | | | | |
| | | Mean | Std. Deviation | Std. Error Mean | Lower | Upper | t | df | Sig. (2-tailed) |
| Pair 1 | HYSPLIT - DATA | -1,93910 | 2,09094 | 0,60360 | -3,26762 | -0,61058 | -3,213 | 11 | 0,008 |

Figure 5. Statistical T-test analysis on concentration HYSPLIT output and Kototabang GAW Monitoring document (Source: Research Result, 2024)

The values obtained from the SPSS T-test indicate that the HYSPLIT model's significant values were less than 0.05, precisely 0.008 ($p < 0.05$). Based on the T-test results, there was a significant difference between the PM2.5 concentrations generated by the HYSPLIT software and the PM2.5 concentrations reported in the Air Quality Monitoring and Forecasting documents from GAW Kototabang.

## Discussion

Several areas were not exposed to volcanic ash dispersion based on HYSPLIT software simulations. Several factors, including meteorological conditions, wind speed, and the topographical characteristics of the region, likely influence this phenomenon. These factors can be explained scientifically as follows:

*Wind Speed and Direction*

Wind parameters are crucial in determining air pollution dispersion patterns, with wind direction influencing the movement of pollutants and wind speed affecting the extent of their spread in the atmosphere. In this study, wind speeds around Mount Marapi during the six simulation days, as shown in Table 2, were generally low, ranging from 0.5 to 2.8 m/s. These relatively calm wind conditions suggest that pollutant dispersion in the study area may have been slow. The direction of the wind during the simulation was opposite to the direction of volcanic ash dispersion, which further influenced the movement of pollutants. According to Rao *et al. (2007),* weak winds can cause pollutants to remain near their source, potentially leading to accumulation in the surrounding area. On February 4, 2024, the highest recorded average wind speed was 1.61 m/s, while the lowest occurred on January 19, 2024, at 0.9 m/s. This variation in wind speed likely influenced the affected areas and the intensity of pollutant accumulation in certain zones. The relatively low variability in wind speed also indicates atmospheric stability, which can lead to higher pollutant concentrations near the emission source, especially under stagnant conditions. Wind speed and direction play an important role in pollutant dispersion, with higher speeds promoting dilution and reducing concentration as pollutants travel further from the source.

*Solar Radiation*

Solar radiation is a key parameter in environmental pollution and climate change studies due to its significant role in influencing temperature and atmospheric processes. According to Table 2, the highest solar radiation around Mount Marapi occurs during the daytime, with values ranging from 0 to 825.6 Wh/m², and the highest average recorded on February 4, 2024. Research by Shresta *et al.* (2019) reveals that solar radiation directly affects air temperature, making it an important factor in atmospheric dynamics. Furthermore, solar radiation is closely related to particles of air pollution. These particles can influence atmospheric transparency and the amount of solar radiation reaching the Earth's surface through reflection and absorption processes. When atmospheric pollutants absorb solar radiation energy, photochemical reactions can occur, transforming these pollutants into toxic substances, as described in Zhang *et al.'s* (2022) research. Thus, solar radiation impacts temperature and triggers chemical processes in the atmosphere that can degrade air quality.

*Mixing Height*

Mixing height in the research location ranges from 250 meters in the early morning to 2000 meters during the day. This variation is closely related to mixing height, also known as mixing depth, which is the height above the ground where pollutants can be dispersed throughout the atmospheric boundary layer. Pollutants emitted from the Earth's surface will rise into the mixing layer, influenced by surface conditions. Depending on atmospheric stability and other factors, this layer spans a certain height, typically ranging from several hundred meters to several kilometers (Ilaboya, 2011). The mixing height is affected by atmospheric stability, where higher mixing heights generally indicate more unstable conditions and a more significant potential for pollutant dispersion. In this case, the observed range of mixing height, from 250 meters in the early morning to 2000 meters in the afternoon, suggests that during the day, more unstable atmospheric conditions facilitate the dispersion of pollutants over a larger area, while at night, the lower mixing height may limit this dispersion.

*Atmospheric Stability*

In the research location, atmospheric stability tends to be higher during the day, with stability conditions rated as f in the early morning and b and c during the day. However, stability returns to the f value at night, indicating that the atmosphere is more stable at night, potentially hindering pollutant dispersion. This atmospheric stability is influenced by vertical air movement, which depends on temperature and atmospheric pressure and subsequently triggers convection or air mixing. Differences in Earth's heating affect air conditions through conduction and convection, causing air to move in three dimensions—horizontal, vertical, and turbulence. Thermal and mechanical turbulence occurs when air moves across barriers or is heated by sunlight. While higher atmospheric stability can enhance pollutant dispersion, mechanical turbulence can hinder airflow, increasing pollutant concentrations (Franek & De Rose, 2003).

One of the input data factors influencing pollutant concentration is the source diameter. The source diameter affects pollutant concentrations in the atmosphere, where a larger crater diameter tends to reduce pollutant concentrations at the ground surface. This occurs because a larger source diameter enhances pollutant dispersion efficiency. A more significant source diameter allows pollutants to mix with a broader air volume, significantly reducing pollutant concentrations at the ground surface (Baturante, 2022; Brink & Crocker, 1964; Lateb *et al.*, 2011).

Besides that, based on the volcanic ash dispersion map generated using HYSPLIT and validated with processed HIMAWARI satellite data, it was concluded that the dispersion modeled using HYSPLIT falls within the coverage of particle dispersion detected by the satellite station. The particle dispersion polygons displayed by HIMAWARI indicate a significantly larger extent than those generated by HYSPLIT and AERMOD. This discrepancy occurs because the satellite captures the distribution of all particles from various pollution sources, including both anthropogenic and natural activities. In contrast, the HYSPLIT model only represents volcanic ash dispersion based on the specific source input, which in this case is Mount Marapi. As shown by Chen *et al.* (2023), along with a comparison of AOD data from Himawari-8 with the aerosol transport and distribution patterns predicted by the HYSPLIT model. This comparison validates the accuracy of the satellite data against the model predictions, demonstrating consistency between the Himawari-8 aerosol data and the HYSPLIT particle distribution results.

Based on the volcanic ash dispersion map generated by HYSPLIT, validated using screenshots from satellite data processing with Himawari 8, it can be concluded that the dispersion obtained from HYSPLIT remains within the range of particle dispersion displayed by the satellite stations. The particle dispersion polygons shown by the Himawari 8 satellite indicate a generally more significant extent than HYSPLIT, as the satellite can capture the entire particle distribution from various anthropogenic and natural pollution sources. In contrast, HYSPLIT modeling only presents volcanic ash dispersion specific to the input source, which is Mount Marapi. The statistical analysis results show a significant difference between the concentrations generated by HYSPLIT and those in the Air Quality Monitoring document from GAW Kototabang. This discrepancy is primarily due to the concentrations in the monitoring data representing an accumulation from various sources or activities, such as traffic, combustion, industrial processes, etc.

## Conclusions

This study analyzed the dispersion patterns of volcanic ash from the eruption of Mount Marapi in West Sumatra using HYSPLIT software, validated with Himawari-8 satellite data and PM2.5 air quality data from the GAW Kototabang station. During the highest eruption on December 3, 2023, the maximum PM2.5 concentration reached 28E-03 mg/m³, while during the smallest eruption on February 4, 2024, the maximum concentration was only 43E-08 mg/m³, indicating that eruption height significantly affects PM2.5 concentrations. The volcanic ash tended to disperse toward Minangkabau International Airport (BIM) during closure periods on December 22, 2023, January 5, 2024, and January 19, 2024. Validation using Himawari-8 data showed that the dispersion patterns generated by HYSPLIT were generally consistent, although the satellite imagery indicated a wider dispersion range due to capturing particles from various sources. PM2.5 concentration analysis revealed significant differences between HYSPLIT results and GAW Kototabang observational data ($\rho < 0.05$), likely due to the observational data representing an accumulation from multiple pollution sources. Meteorological factors influenced the volcanic ash dispersion patterns, including low wind speeds (0.5–2.8 m/s), prevailing wind direction, solar radiation, and mixing layer height. This study recommends prioritizing mitigation measures in volcanic ash hazard zones within a 0–10 km radius of the crater, including activity restrictions and evacuation route planning. HYSPLIT was deemed adequate for simulating volcanic ash dispersion, although enhancing meteorological input data is necessary to improve accuracy. The findings of this study are expected to serve as a foundation for developing early warning systems and more effective disaster mitigation measures to manage the impacts of volcanic eruptions on communities and the environment.

## Acknowledgments

Technology and Community Service (DRTPM) Directorate General of Higher Education, Research and Technology (Ditjen Diktiristek) Ministry of Education, Culture, Research and Technology (Kemendikbudristek), under contract No. 041/E5/PG.02.00.PL/2024. We want to thank Global Atmospheric Watch (GAW) Kototabang Station for their cooperation in providing data for this research.

## References

Angell, J. K., Pack, D. H., Machta, L., Dickson, C. R., & Hoecker, W. H. (1972). Three-dimensional air trajectories determined from tetroon flights in the planetary boundary layer of the Los Angeles Basin. *Journal of Applied Meteorology, 11*(3), 451–471. http://www.jstor.org/stable/26175739.

Arya, S. P. (2005). Micrometeorology and atmospheric boundary layer. *Pure and Applied Geophysics*, *162*, 1721-1745.

Baturante, N. (2022). Pengaruh Tinggi Dan Diameter Cerobong Pltu Terhadap Dispersi SO2 Di Udara Menggunakan Model Gaussian Plume. *Jurnal Pendidikan Kimia Unkhair (JPKU)*, *2*(1). Https://Doi.Org/10.33387/Jpku.V2i1.4952

Brink, J. A., & Crocker, B. B. (1964). Practical Applications Of Stacks To Minimize Pollution Problems. *Journal Of The Air Pollution Control Association*, *14*(11), 449–454. Https://Doi.Org/10.1080/00022470.1964.10468312

Cashman, K., & Rust, A. (2016). Introduction: Part 2: Volcanic Ash: Generation And Spatial Variations. In *Volcanic Ash: Hazard Observation* (Pp. 5-22). Https://Doi.Org/10.1016/B978-0-08-100405-0.00002-1

Center for Volcanology and Geological Disaster Mitigation (PVMBG). (2024). Announcement of the increase in the activity level of Mount Marapi, West Sumatra, from Level II (Alert) to Level III (Alert) 2024. Center for Volcanology and Geological Disaster Mitigation.

Center for Volcanology and Geological Disaster Mitigation (PVMBG). (2023). Mount Marapi Activity Report. Center for Volcanology and Geological Disaster Mitigation.

Chandra, B. (2006). Introduction Environmental Health (EGC: Jakarta).

Chai, T., Crawford, A., Stunder, B., Pavolonis, M. J., Draxler, R., & Stein, A. (2017). Improving volcanic ash predictions with the HYSPLIT dispersion model by assimilating MODIS satellite retrievals. *Atmospheric Chemistry and Physics*, *17*(4), 2865-2879. https://doi.org/10.5194/acp-17-2865-2017

Chen, S. P., Lu, C. H. S., Davies, J. E., Ou-Yang, C. F., Lin, N. H., Huff, A. K., ... & Wang, J. L. (2023). Infusing satellite data into aerosol forecast for near real-time episode detection and diagnosis in East Asia. *Science of The Total Environment*, *856*, 158797. https://doi.org/10.1016/j.scitotenv.2022.158797

Directorate General of Civil Aviation (DJPU). (2024). *Public information* [Website]. Retrieved July 21, 2024, from https://hubud.dephub.go.id/hubud/website/search?q=erupsi+gunung+berapi

Draxler, R. R., & Hess, G. D. (1998). An overview of the HYSPLIT_4 modelling system for trajectories. *Australian meteorological magazine*, *47*(4), 295-308. https://www.arl.noaa.gov/documents/reports/MetMag.pdf

Ministry of Energy and Mineral Resources (ESDM). (2023). *Press Release Marapi Eruption 3 December 2023*. Retrieved from https://geologi.esdm.go.id/media-center/press-release-erupsigunungmarapisumaterabarat3desember2023#:~:text=Perkembangan%20terakhir%20aktivitas%20G.%20Marapi,m%20di%20atas%20permukaan%20laut).

Ministry of Energy and Mineral Resources (ESDM). (2023-2024). *MAGMA Indonesia*. Retrieved from https://magma.esdm.go.id/v1/gunung-api/informasi-letusan

Fleming, Z. L., Monks, P. S., & Manning, A. J. (2012). Untangling the influence of air-mass history in interpreting observed atmospheric composition. *Atmospheric Research*, *104*, 1-39. http://dx.doi.org/10.1016/j.atmosres.2011.09.009

Franek, W., & DeRose, L. (2003). Principles and Practices of Air Pollution Control and Analysis. United States: Environmental Protection Agency.

Global Monitoring Station (GAW) Koto Tabang. (2023–2024). *Monitoring and forecasting document of air quality parameters for PM2.5 and PM10*. Agam: Global Atmospheric Watch Station (GAW) Bukit Koto Tabang.

Hamdiyessi, S., Marzuki, M., Putra, A., & Indrastuti, N. (2022). Analysis of volcanic earthquake hypocenter distribution of Mount Marapi using Geiger's method with adaptive damping (GAD). *Jurnal Fisika Unand, 11*(4), 414–420. https://doi.org/10.25077/jfu.11.4.414-420.2022

Hemond, H. F., & Fechner, E. J. (2022). *Chemical fate and transport in the environment*. academic press.

Horwell, C. J., Baxter, P. J., Hillman, S. E., Calkins, J. A., Damby, D. E., Delmelle, P., ... & Tomatis, M. (2013). Physicochemical and toxicological profiling of ash from the 2010 and 2011 eruptions of Eyjafjallajökull and Grímsvötn volcanoes, Iceland using a rapid respiratory hazard assessment protocol. *Environmental Research*, *127*, 63-73. https://doi.org/10.1016/j.envres.2013.08.011

Ilaboya, I. R., Atikpo, E., Umukoro, L., Omofuma, F. E., & Ezugwu, M. O. (2011). *Analysis Of The Effects Of Mixing Height And Other Associated Factor*.

Iqbal, M., Denhi, A. D. A., Kristianto, & Prayoga, A. (2023). Morphological analysis of Anak Krakatau Volcano after the 22 December 2018 eruption using differential interferometry synthetic aperture radar (DInSAR). *Journal of Geoscience, Engineering, Environment, and Technology, 8*(2), 90–98. https://doi.org/10.25299/jgeet.2023.8.2.11651

Ishii, K., Hayashi, Y., & Shimbori, T. (2018). Using Himawari-8, estimation of $SO_2$ cloud altitude at Aso volcano eruption on October 8, 2016. *Earth, Planets and Space.* https://doi.org/10.1186/s40623-018-0793-9

Japan Aerospace Exploration Agency Earth Observation Research Center (JAXA EORC). (2023-2024). *Himawari Monitor Aerosol Products*. Retrieved from https://www.eorc.jaxa.jp/ptree/index.html

Japan Aerospace Exploration Agency Earth Observation Research Center (JAXA EORC). (2018). *Himawari Monitor Aerosol Products*. https://www.eorc.jaxa.jp/ptree/documents/Himawari_Monitor_Aerosol_Product_v5.pdf

Kahl, J. D., & Chapman, H. L. (2018). Atmospheric stability characterization using the Pasquill method: A critical evaluation. *Atmospheric Environment*, *187*, 196-209. http://dx.doi.org/10.1016/j.atmosenv.2018.05.058

Lateb, M., Masson, C., Stathopoulos, T., & Bédard, C. (2011). Effect Of Stack Height And Exhaust Velocity On Pollutant Dispersion In The Wake Of A Building. *Atmospheric Environment*, *45*(29), 5150–5163. Https://Doi.Org/10.1016/J.Atmosenv.2011.06.040

Lee, S.-K., Ryu, G.-H., Hwang, E.-H., Choi, J.-K., & Lee, C.-W. (2014). Predicting the extent of volcanic ash dispersion using GOCI images and the HYSPLIT model: A case study of the 17 September 2013 eruption at Sakurajima Volcano. *Korean Journal of Remote Sensing, 30*(2), 303–314. https://doi.org/10.7780/kjrs.2014.30.2.12

Mastin, L. G. (2014). Testing The Accuracy Of A 1-D Volcanic Plume Model In Estimating Mass Eruption Rate. *Journal Of Geophysical Research: Atmospheres*, *119*(5), 2474-2495. Https://Doi.Org/10.1002/2013JD020604

Mastin, L. G., Guffanti, M., Servranckx, R., Webley, P., Barsotti, S., Dean, K., ... & Waythomas, C. F. (2009). A multidisciplinary effort to assign realistic source parameters to models of volcanic ash-cloud transport and dispersion during eruptions. *Journal of volcanology and Geothermal Research*, *186*(1-2), 10-21. https://doi.org/10.1016/j.jvolgeores.2009.01.008

NASA Langley Research Center. (Nd.). NASA POWER Data Access Viewer. NASA. https://power.larc.nasa.gov

Putra, D. E., & Sitanala, F. T. R. (2016). Risiko erupsi Gunung Marapi di Kabupaten Tanah Datar. *Jurnal Geosains Terapan*, *2*(3), 7-7. https://lib.ui.ac.id/detail?id=20412950&lokasi=lokal

Rao, C. S. (2007). *Environmental pollution control engineering*. New Age International.

Regulations of the Governor of West Sumatra. (2016). *Contingency plan and standard operating procedure for volcanic disasters in West Sumatra Province*.

Rodell, M., Houser, P. R., Jambor, U. E. A., Gottschalck, J., Mitchell, K., Meng, C. J., ... & Toll, D. (2004). The global land data assimilation system. *Bulletin of the American Meteorological society*, *85*(3), 381-394. http://dx.doi.org/10.1175/BAMS-85-3-381

Shrestha, A. K., Thapa, A., & Gautam, H. (2019). Solar Radiation, Air Temperature, Relative Humidity, and Dew Point Study: Damak, Jhapa, Nepal. International Journal of Photoenergy, 2019. https://doi.org/10.1155/2019/8369231

Stein, A. F., Draxler, R. R., Rolph, G. D., Stunder, B. J. B., Cohen, M. D., & Ngan, F. (2015). NOAA's HYSPLIT atmospheric transport and dispersion modeling system. *Bulletin of the American Meteorological Society*. https://doi.org/10.1175/BAMS-D-14-00110.1

Su, L., Yuan, Z., Fung, J. C., & Lau, A. K. (2015). A comparison of HYSPLIT backward trajectories generated from two GDAS datasets. *Science of the Total Environment*, *506*, 527-537. https://doi.org/10.1016/j.scitotenv.2014.11.072

Suhendro, I., Isnain, M. N., & Wahyudi, R. (2022). Rock characteristics of post-caldera volcanoes in Dieng volcanic complex (DVC), Central Java, Indonesia. *Journal of Geoscience, Engineering, Environment, and Technology, 7*(4), 151–157. https://doi.org/10.25299/jgeet.2022.7.4.10015

Zhang, X., Zhang, M., Cui, Y., & He, Y. (2022). Estimation Of Daily Ground-Received Global Solar Radiation Using Air Pollutant Data. *Frontiers In Public Health*, *10*, 860107. Https://Doi.Org/10.3389/Fpubh.2022.860107